

9170  
NACA TN 2835

# NATIONAL ADVISORY COMMITTEE FOR AERONAUTICS



TECH LIBRARY KAFB, NM

TECHNICAL NOTE 2835

## EFFECT OF CHANGING PASSAGE CONFIGURATION ON INTERNAL-FLOW CHARACTERISTICS OF A 48-INCH CENTRIFUGAL COMPRESSOR

### II - CHANGE IN HUB SHAPE

By John Mizisin and Donald J. Michel

Lewis Flight Propulsion Laboratory  
Cleveland, Ohio



Washington  
November 1952

AFMDC  
TECHNICAL LIBRARY

AFMDC  
TECHNICAL LIBRARY



0065824

1G

## NATIONAL ADVISORY COMMITTEE FOR AERONAUTICS

## TECHNICAL NOTE 2835

## EFFECT OF CHANGING PASSAGE CONFIGURATION ON INTERNAL-FLOW

2674

## CHARACTERISTICS OF A 48-INCH CENTRIFUGAL COMPRESSOR

## II - CHANGE IN HUB SHAPE

By John Mizisin and Donald J. Michel

## SUMMARY

The passage contour of a 48-inch centrifugal compressor was modified by changing the shape of the hub to control deceleration rates along the blade surfaces in order to improve the internal efficiency of the impeller. A comparison of internal-flow characteristics at design flow rate was made with the original impeller and with a previously investigated modified-blade impeller that had the same area variation in the passage. In addition, flow characteristics of the modified-hub impeller over a flow range from maximum flow to near surge at a corrected tip speed of 700 feet per second are presented.

At design flow, even though the deceleration rate along the trailing face was less for the modified-hub impeller than for the original impeller, the clearance losses (increased by the larger ratio of clearance to passage height) caused the total-pressure losses (and thus the relative adiabatic efficiency) to be about the same at the impeller exit for the two configurations, thus precluding any improvement in over-all performance. As in the original and modified-blade impellers, large losses occurred at the driving-face inlet at negative angles of attack and in regions of large decelerations along the trailing-face flow surface.

## INTRODUCTION

The results of previous experimental investigations of flow characteristics within the rotating impeller channel conducted at the NACA Lewis laboratory have shown that large losses occurred near flow surfaces with large deceleration rates (references 1 and 2). When the deceleration rates were controlled by modifying the blade shape (reference 3), the internal relative adiabatic efficiency was improved although no improvement was found in over-all compressor efficiency because of the inefficient blade-exit form. It was believed that a similar high internal efficiency along with improved over-all compressor efficiency

might be realized by modifying the hub to reduce the deceleration ratio along the flow surface and eliminating the thick blunt blade tip. On the other hand, the internal efficiency might be reduced because of the poorer aspect ratio of the passage.

The present investigation was conducted in order to estimate the relative magnitude of the previously discussed effects. A comparison of the internal-flow characteristics within the rotating passage of the modified-hub impeller with those of the original impeller and the modified-blade impeller at the design flow rate is presented herein. Flow characteristics over the entire weight-flow range for the modified-hub impeller will also be presented.

2674

The compressor was operated over the weight-flow range from maximum flow to near surge at a corrected tip speed of 700 feet per second. Experimental efficiencies, pressure-loss contours, velocities, and pressures are compared for the three impeller configurations at design flow rate, and efficiency and velocity contours are shown for the modified-hub impeller at several weight flows.

#### APPARATUS

The modified-hub impeller used in the experimental investigation is shown in figure 1. Balsa wood was glued to the impeller hub to modify the blade height. (The dark area in the photograph of the impeller passage is the balsa modification.) The area variation of the modified-hub impeller (area normal to the radial velocity component at corresponding radii) was the same as that for the modified-blade impeller. The modification started at about the 16-inch radius and continued to the exit. The original blade shape and shroud contour were unchanged. Figure 2 shows a schematic view of the modified passage in the hub-shroud plane. The pertinent passage data for the modified-hub impeller are presented in table I. In this table, blade thickness was corrected to an average thickness so that the actual passage area at any radius could be computed from the blade height and the number of blades (18) without consideration of blade taper.

Because the impeller hub contour was changed, the diffuser was modified to give smooth flow conditions at the diffuser inlet by the placing of wood of the desired thickness at the rear diffuser surface. In changing the passage width, the diffuser was no longer a constant-area type, but it became slightly convergent. Because of the decrease in diffuser passage width, the diffuser instruments were changed from four- to three-probe pressure and thermocouple rakes. The total-pressure rakes were of the shielded type and the thermocouples were of the calibrated bare-wire spike type. With these exceptions, over-all instrumentation remained the same as reported in reference 2.

Since the impeller passage height was modified by changing the hub shape beyond the 16-inch radius, the total-pressure probes in the rotating passage beyond that radius were no longer at the passage midheight but were closer to the hub. These probes were of the Kiel type. Static pressures were measured along the hub through 0.030-inch-diameter orifices as was done in the previous impellers. The pressure-transfer device was of the sealed ball-bearing type. A complete description of the impeller instrumentation and pressure-transfer device is given in reference 2.

2674

### PROCEDURE

The compressor was operated over a weight-flow range from a maximum corrected weight flow  $W\sqrt{\theta}/\delta$  of 43 pounds per second to near surge at 12.5 pounds per second at a corrected tip speed  $U/\sqrt{\theta}$  of 700 feet per second. (All symbols are defined in the appendix.) The operating procedure was the same as described in reference 2.

The experimental efficiencies and velocities were computed by the method given in reference 1.

## RESULTS AND DISCUSSION

### Over-All Performance

The over-all pressure ratio in the modified-hub impeller was slightly lower than that of the original impeller, as shown in figure 3. The peak pressure ratio was 1.444 for the modified-hub impeller as compared with 1.455 for the original impeller and the peak adiabatic efficiency (fig. 4) was 0.78 for the modified-hub impeller as compared with 0.80 for the original impeller. The efficiency of the modified-hub impeller was probably lower than that of the original impeller because of the greater effect of clearance losses and because of the closer spacing of the diffuser walls which made a larger ratio of wetted surface to flow area even though the flow path was shortened by higher radial exit velocities (reference 4).

The surge point occurred at a lower weight flow in the modified-hub impeller possibly because the higher relative velocity throughout the passage caused the eddy to form at a lower weight flow than in the original impeller (reference 5).

### Comparison of Internal-Flow Characteristics of Three Impeller Configurations at Design Flow Rate

The comparisons of flow characteristics within the rotating impeller channel for the three impeller configurations are shown in

figures 5 to 10 for the design flow rate of 26 pounds per second. The total-pressure-loss contours (fig. 5) show that at the impeller exit the losses were about the same for both the original and modified-hub impellers. The original impeller had local peak losses greater than those of both the modified-blade and modified-hub impellers at the  $22\frac{1}{2}$ -inch radius.

A fair comparison could not be made beyond that point because the cut back of the modified blades caused poor flow conditions. The total-pressure losses in the modified-hub impeller occurred farther downstream in the passage than in the original impeller, but losses at the exit of about the same magnitude also resulted. Larger clearance losses occurred in the modified-hub impeller because of the increased leakage through the clearance space (0.070-in. clearance) which influenced the main flow stream near the trailing face. For a given clearance space, the clearance leakage losses increase with reduced blade height because of the accompanying increase in blade loading, which results in a greater pressure difference across the clearance. If the total pressure had been measured at the passage midheight instead of near the hub, the losses might possibly have been greater; reference 6 indicates that the flow near the impeller exit was improved as the hub was approached.

The relative adiabatic efficiency contours are shown in figure 6. The patterns shown are quite similar to the total-pressure-loss contours. The relative efficiency at the exit of the modified-hub impeller was about the same as that for the original impeller, even though the efficiency was generally greater throughout the remainder of the passage. The efficiency along the trailing face of the modified-hub impeller was lower than that of the modified-blade impeller, indicating greater losses due to leakage through the clearance space. Figure 7 shows the average adiabatic efficiency across the passage at various radii for the three impeller configurations. The average efficiency of the modified-hub impeller was higher than that of the original impeller throughout most of the passage, but was lower than the modified-blade impeller efficiency. At the exit, however, total-pressure losses reduced the efficiency to that of the original impeller. The efficiency of the modified-blade impeller was not shown near the exit because the cut-back blade caused poor flow conditions as discussed previously.

The static-pressure distribution near the blade surfaces (fig. 8) indicates that the blade loading is greater for the modified-hub impeller than for the original impeller. This increased blade loading is necessary to maintain the same impeller torque with the decreased blade height.

A comparison of the relative velocity throughout the passage and near the blade surfaces for the three impeller configurations is shown in figures 9 and 10. The deceleration rates were decreased along the trailing face for the modified-hub impeller as compared with the original

2674  
impeller. However, even though the velocity pattern is good along that flow surface, the relative efficiency is lower because of losses caused by leakage through the clearance. The average velocity across the passage at any radius is about the same for both modifications up to about the  $22\frac{1}{2}$ -inch radius. Beyond this value, since the passage areas are no longer equal, the velocity distribution differs. Any discrepancies in velocity distribution are probably due to a different boundary-layer formation arising from different flow conditions in the passage.

The velocity and efficiency differences that exist between the original and modified impellers in the part of the passage where no alteration was made (12- to 16-in. radius, figs. 6 and 9) are probably due to a preadjustment to a new flow angle in that section for the modified-hub and -blade impellers. In the original impeller, separation from the trailing face probably caused the air to flow more toward the driving face than along the normal flow path, while for the modified-blade impeller, the blade shape on the driving face would cause the air to be turned more toward the trailing face. With the modified-hub impeller, however, there was probably no separation from the trailing face because of the better flow conditions along that surface; thus the flow would follow some mean path, resulting in different flow conditions in the first part of the passage.

In the last portion of the passage where the blades are nearly radial and at flow rates near design (26 lb/sec), there was fair qualitative agreement with the theoretical velocity pattern for straight radial blades as shown in figure 8(f) of reference 5. The same sort of velocity distribution with a saddle point near the exit occurred in the modified-hub impeller as in the theoretical case.

On the basis of the preceding results, potential increases in impeller efficiency obtained by improved velocity distributions resulting from reduced blade height tend to be balanced by increased leakage losses through the clearance space.

#### Variation of Internal-Flow Characteristics of Modified-Hub

##### Impeller with Weight Flow

The same sources of losses occurred in the modified-hub impeller as in the modified-blade and original impellers as the angle of attack on the blade was changed over the weight-flow range as presented in figures 11 and 12. At large negative angles of attack (figs. 11(a) to 11(d) and 12(a) to 12(d)), large separation losses at the driving-face inlet due to the sharp leading edge existed, whereas for the positive angles

of attack (figs. 11(e) to 11(h) and 12(e) to 12(h)), there were only slight losses because the blade shape better accommodated the flow.

Over the whole range of flow rates, the relative efficiency (and thus the magnitude of losses at the exit (fig. 11)) was about the same as for the original impeller (reference 1) at approximately corresponding flow rates. This similarity resulted because although the losses due to decelerations along the flow surfaces were less in the modified-hub impeller, the losses caused by the flow through the clearance space were greater.

#### SUMMARY OF RESULTS

The following results were obtained in an investigation of the flow within the rotating passages of a 48-inch centrifugal impeller when modified by changing the hub shape:

1. Even though the deceleration rates along the flow surfaces were less in the modified-hub impeller than in the original impeller, the clearance losses (increased by the greater ratio of clearance to blade height) caused the total-pressure losses (and thus the relative efficiency) to be about the same at the impeller exit for the two configurations, thus precluding any improvement in over-all performance.
2. As with the original and modified-blade impellers, large losses occurred at the driving-face inlet at negative angles of attack and in regions of large decelerations along the trailing-face flow surface.

Lewis Flight Propulsion Laboratory  
National Advisory Committee for Aeronautics  
Cleveland, Ohio, August 22, 1952

2674

## APPENDIX - SYMBOLS

The following symbols were used in this report:

|             |   |
|-------------|---|
| $c_0$       | stagnation speed of sound upstream of impeller, ft/sec                    |
| P           | total pressure  |
| $\Delta P$  | total-pressure loss   |
| p           | static pressure   |
| q           | stream velocity, ft/sec   |
| U           | impeller tip speed, ft/sec  |
| W           | weight flow, lb/sec   |
| $\delta$    | ratio of actual inlet total pressure to standard sea-level pressure       |
| $\eta_{ad}$ | adiabatic efficiency  |
| $\theta$    | ratio of actual inlet total temperature to standard sea-level temperature |

Subscripts:

|   |                            |
|---|----------------------------|
| 0 | inlet measuring station    |
| 2 | diffuser measuring station |
| r | relative to impeller       |

## REFERENCES

1. Prian, Vasily D., and Michel, Donald J.: An Analysis of Flow in Rotating Passage of Large Radial-Inlet Centrifugal Compressor at Tip Speed of 700 Feet Per Second. NACA TN 2584, 1951.
2. Michel, Donald J., Ginsburg, Ambrose, and Mizisin, John: Experimental Investigation of Flow in the Rotating Passages of a 48-Inch Impeller at Low Tip Speeds. NACA RM E51D20, 1951.
3. Michel, Donald J., Mizisin, John, and Prian, Vasily D.: Effect of Changing Passage Configuration on Internal-Flow Characteristics of a 48-Inch Centrifugal Compressor. I - Change in Blade Shape. NACA TN 2706, 1952.

4. Stanitz, John D.: One-Dimensional Compressible Flow in Vaneless Diffusers of Radial- and Mixed-Flow Centrifugal Compressors, Including Effects of Friction, Heat Transfer, and Area Change. NACA TN 2610, 1952.
5. Stanitz, John D., and Ellis, Gaylord O.: Two-Dimensional Compressible Flow in Centrifugal Compressors with Straight Blades. NACA TR 954, 1950.
6. Hamrick, Joseph T., and Mizisin, John: Investigation of Flow Fluctuations at the Exit of a Radial-Flow Centrifugal Compressor. NACA RM E52H11, 1952.

2674

2674

TABLE I - BLADE DATA AT MEAN HEIGHT



| Radius<br>(in.) | Blade<br>angle<br>(deg) | Total<br>blade<br>height<br>(in.) | Circumferential<br>thickness, (in.) |           |
|-----------------|-------------------------|-----------------------------------|-------------------------------------|-----------|
|                 |                         |                                   | Actual                              | Corrected |
| 12.3            | 57.7                    | 3.30                              | 0.730                               | 0.897     |
| 13.0            | 55.3                    | 3.05                              | .714                                | .873      |
| 14.0            | 50.9                    | 2.72                              | .665                                | .817      |
| 16.0            | 37.3                    | 2.19                              | .531                                | .654      |
| 18.0            | 20.0                    | 1.62                              | .445                                | .545      |
| 20.0            | 4.0                     | 1.31                              | .410                                | .504      |
| 21.5            | 0                       | 1.15                              | .397                                | .487      |
| 22.5            | 0                       | 1.07                              | .389                                | .478      |
| 23.5            | 4.4                     | 1.02                              | .380                                | .467      |



Figure 1. - Modified impeller used in investigation of flow within rotating passage.

2674

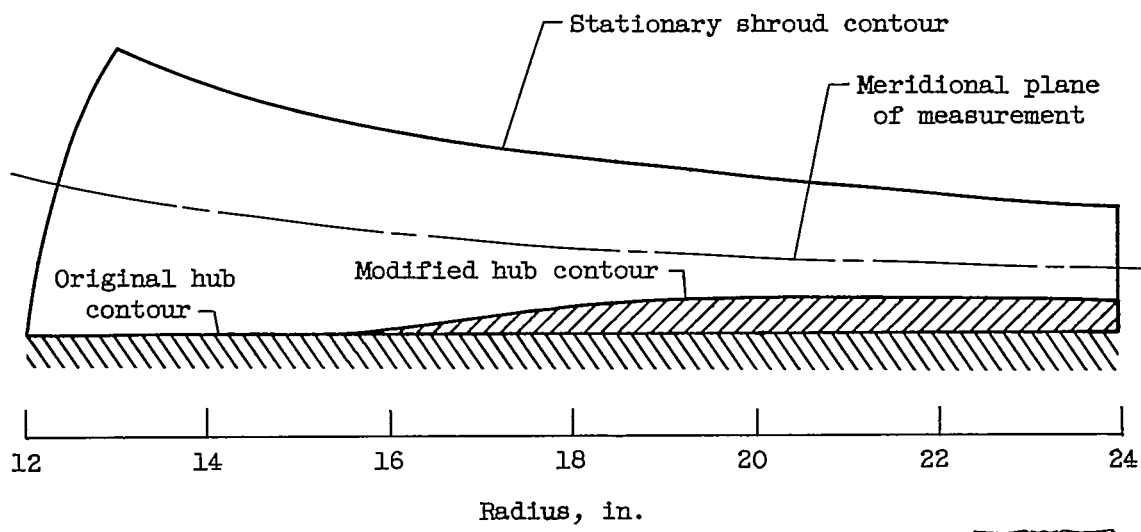


Figure 2. - Comparison of original and modified hub contours.

2674

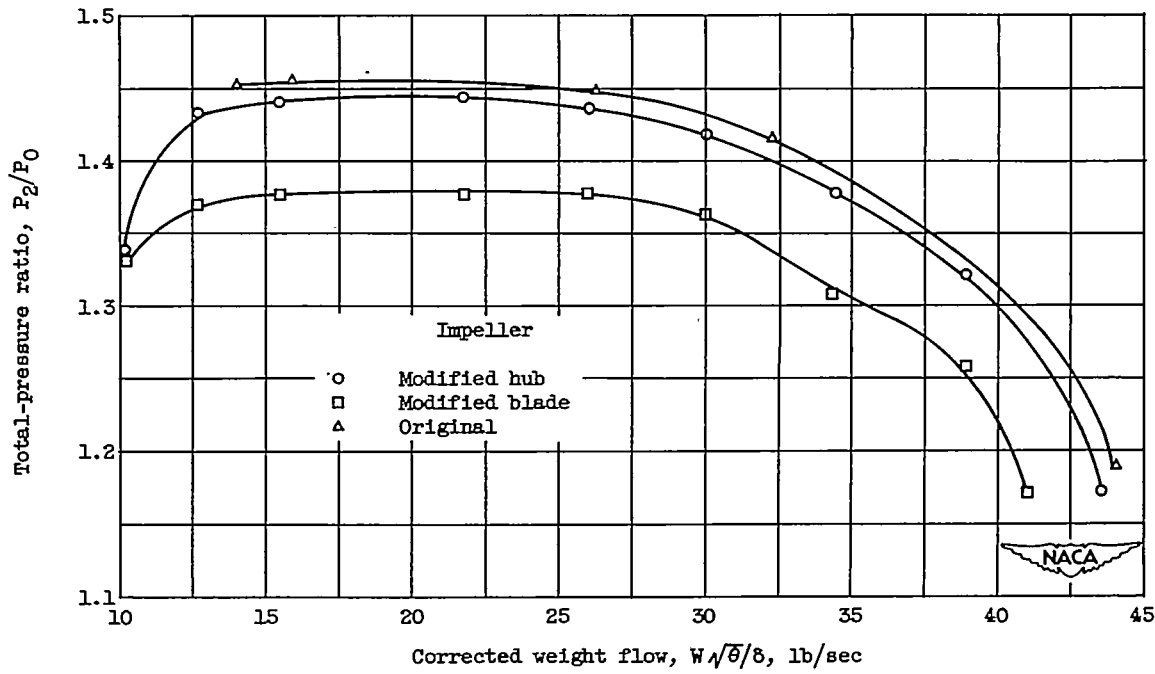


Figure 3. - Total-pressure ratio through impeller based on conditions at diffuser tip ( $1\frac{1}{2}$  impeller rad) for three impeller configurations. Corrected tip speed, 700 feet per second.

2674

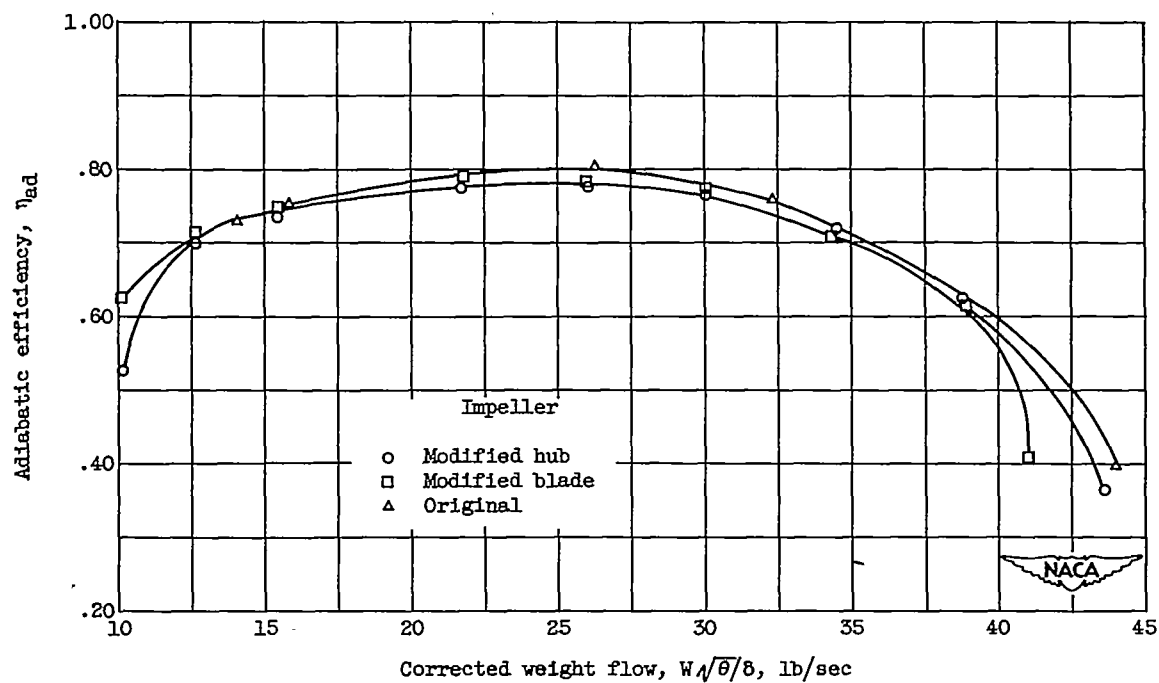
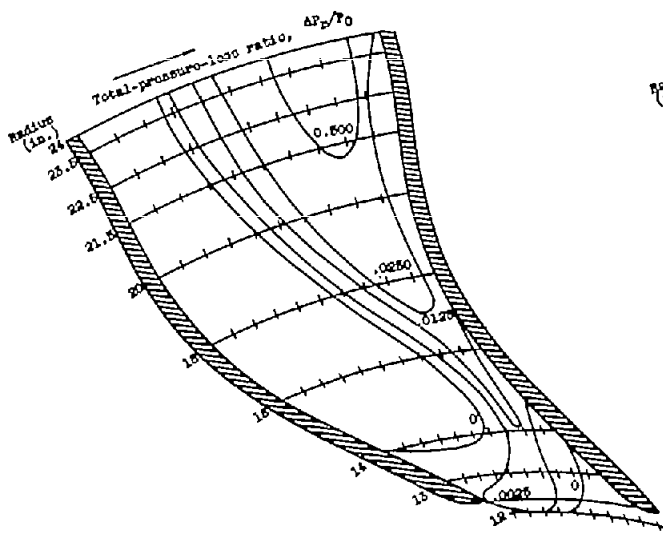
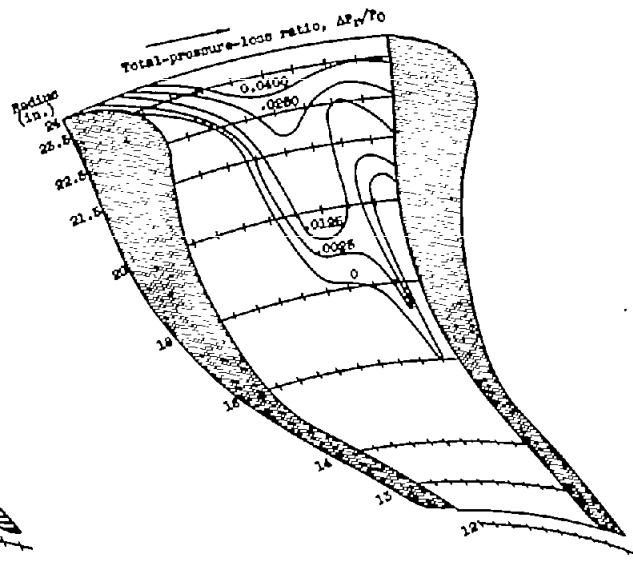


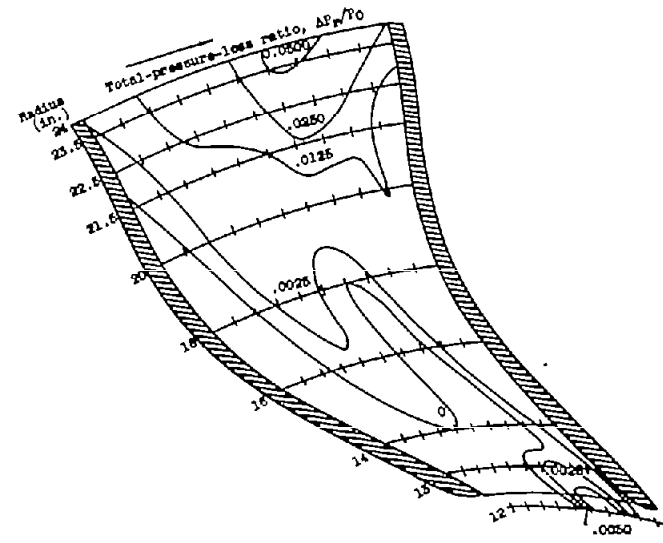
Figure 4. - Adiabatic efficiency of impeller and diffuser based on conditions at diffuser tip ( $1\frac{1}{2}$  impeller rad) for three impeller configurations. Corrected tip speed, 700 feet per second.



(a) Original impeller.

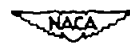


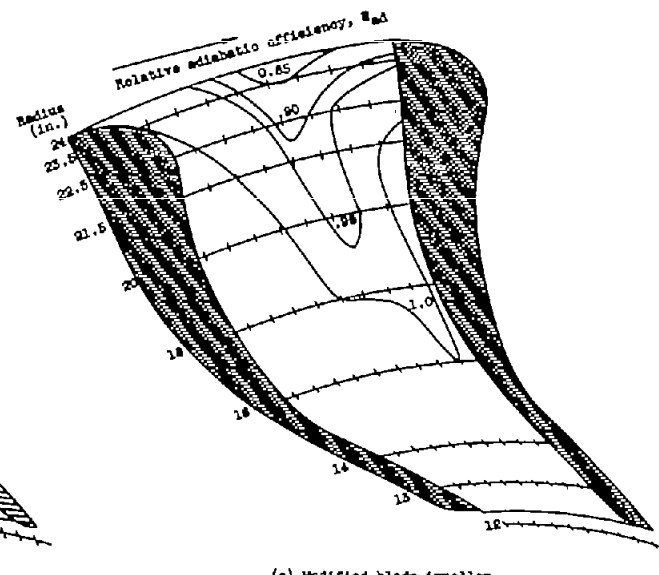
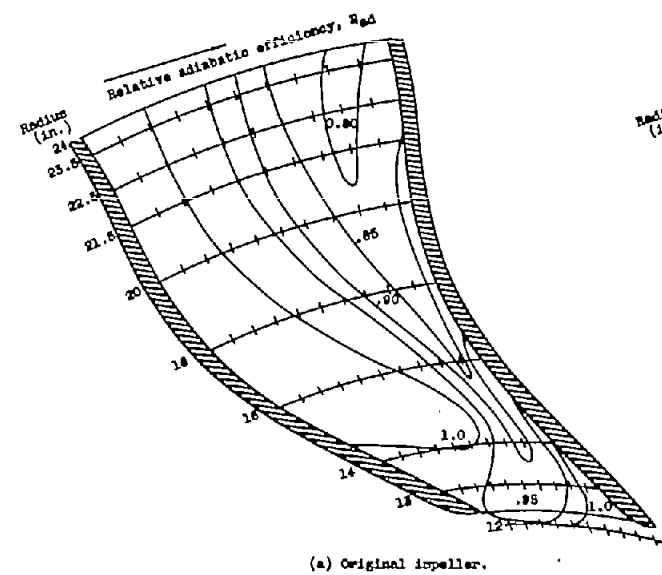
(c) Modified-blade impeller.



(b) Modified-hub impeller.

Figure 5. - Total-pressure-loss distribution throughout impeller rotating passage at corrected weight flow of 26 pounds per second.





NACA

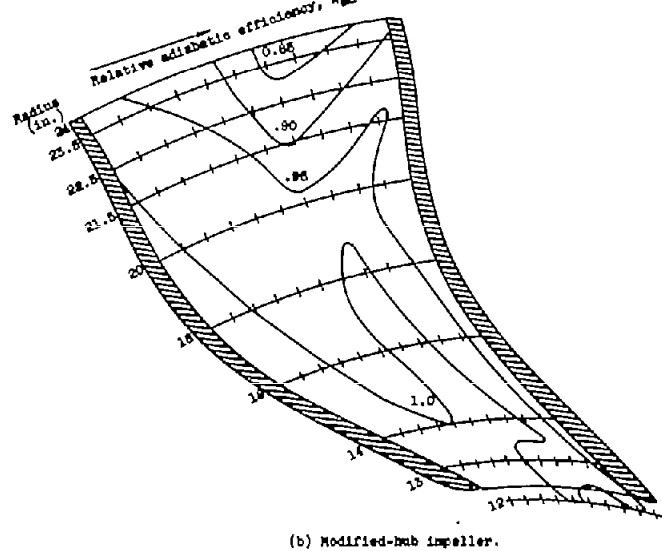


Figure 6. - Relative adiabatic efficiency distribution throughout impeller rotating passage at corrected weight flow of 26 pounds per second.

2674

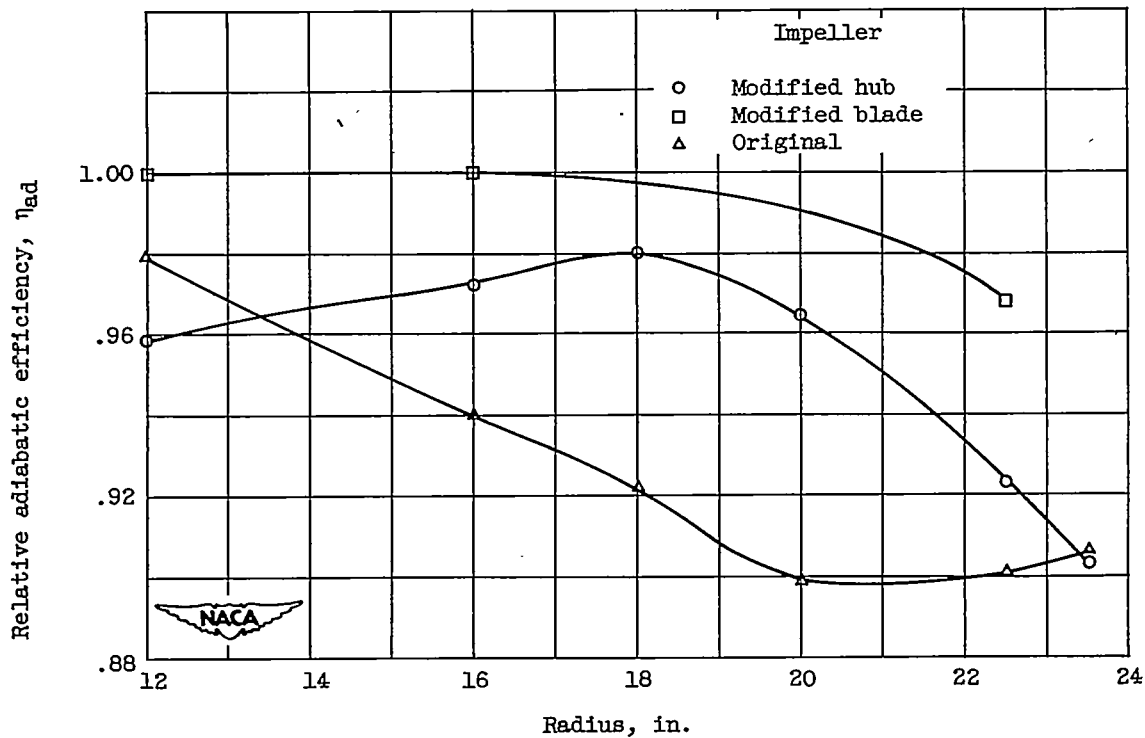


Figure 7. - Average relative adiabatic efficiency across passage at various radii for three impeller configurations at corrected weight flow of 26 pounds per second.

VLSG

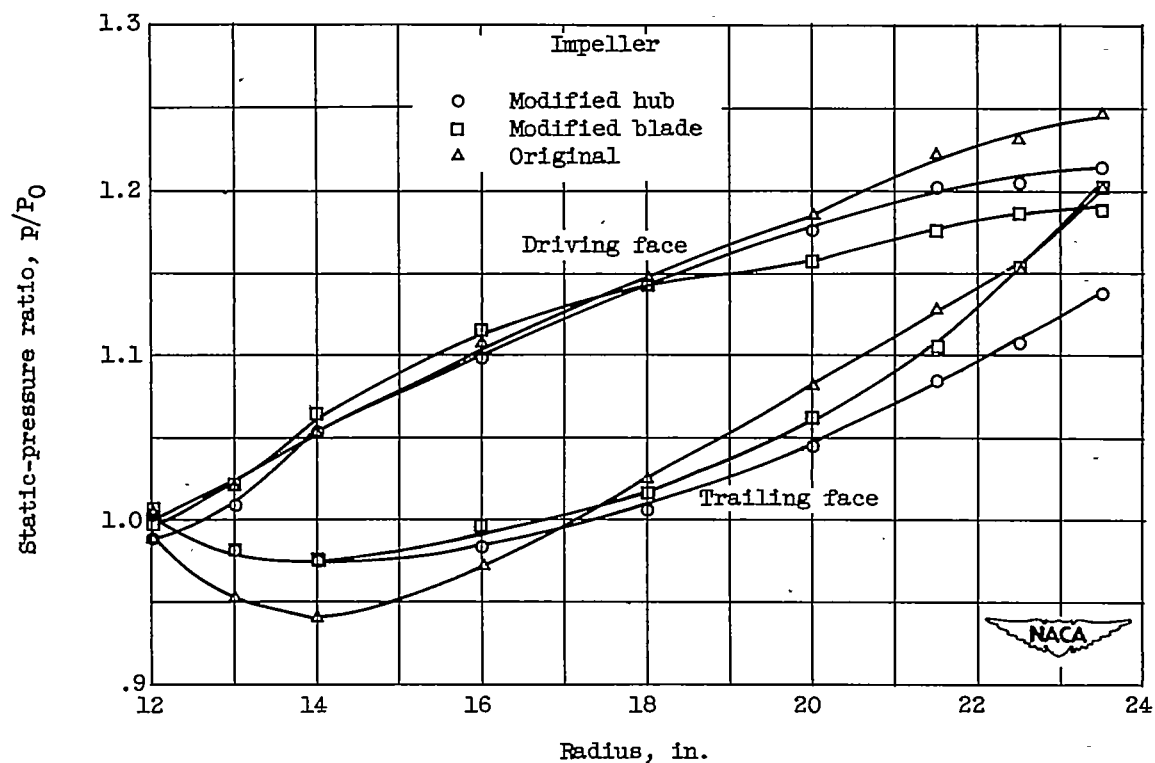
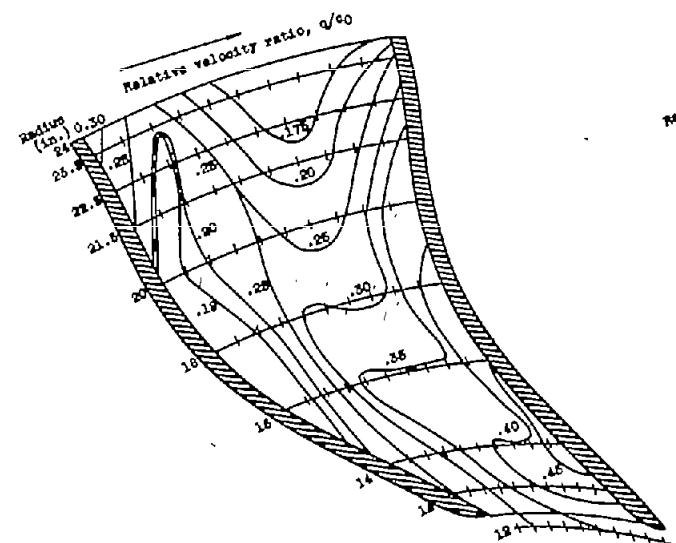
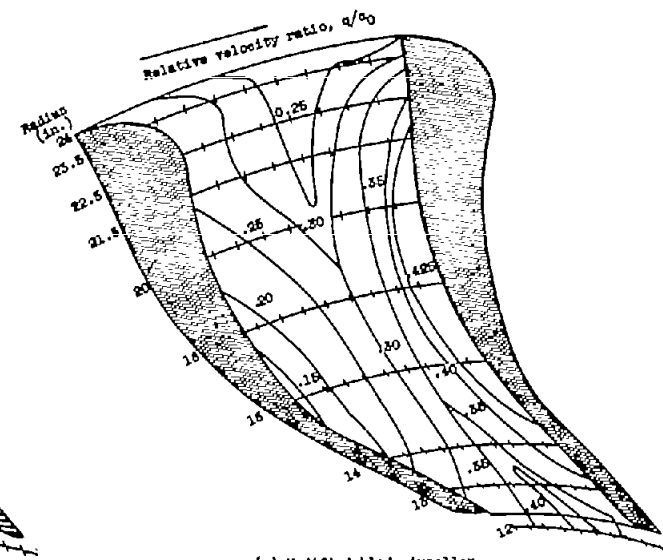


Figure 8. - Static-pressure distribution near blade surfaces for three impeller configurations at corrected weight flow of 26 pounds per second.



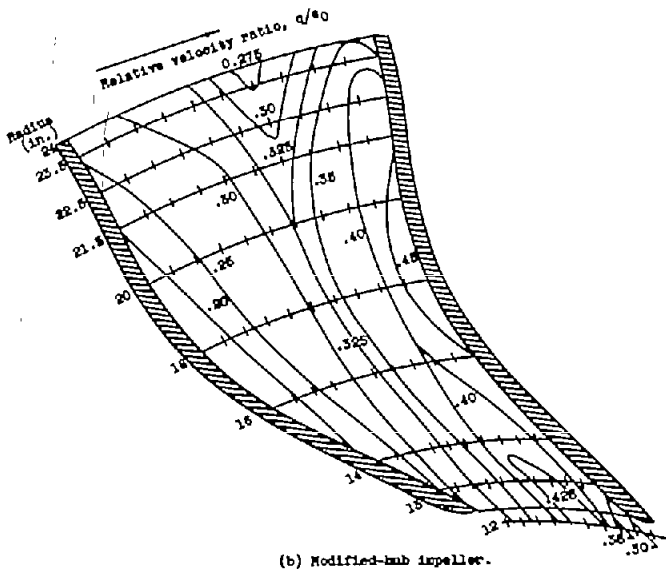
(a) Original impeller.



(c) Modified blade impeller.



Figure 9. - Relative velocity distribution throughout impeller rotating passage at corrected weight flow of 26 pounds per second.



(b) Modified-hub impeller.

2674

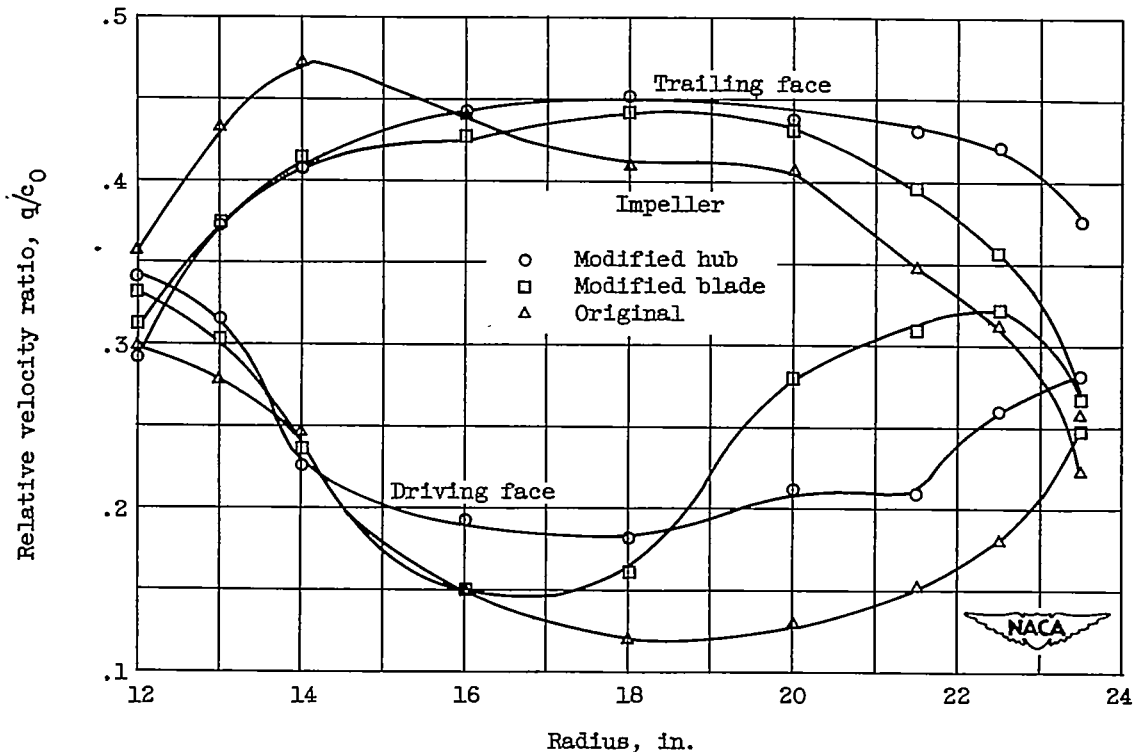
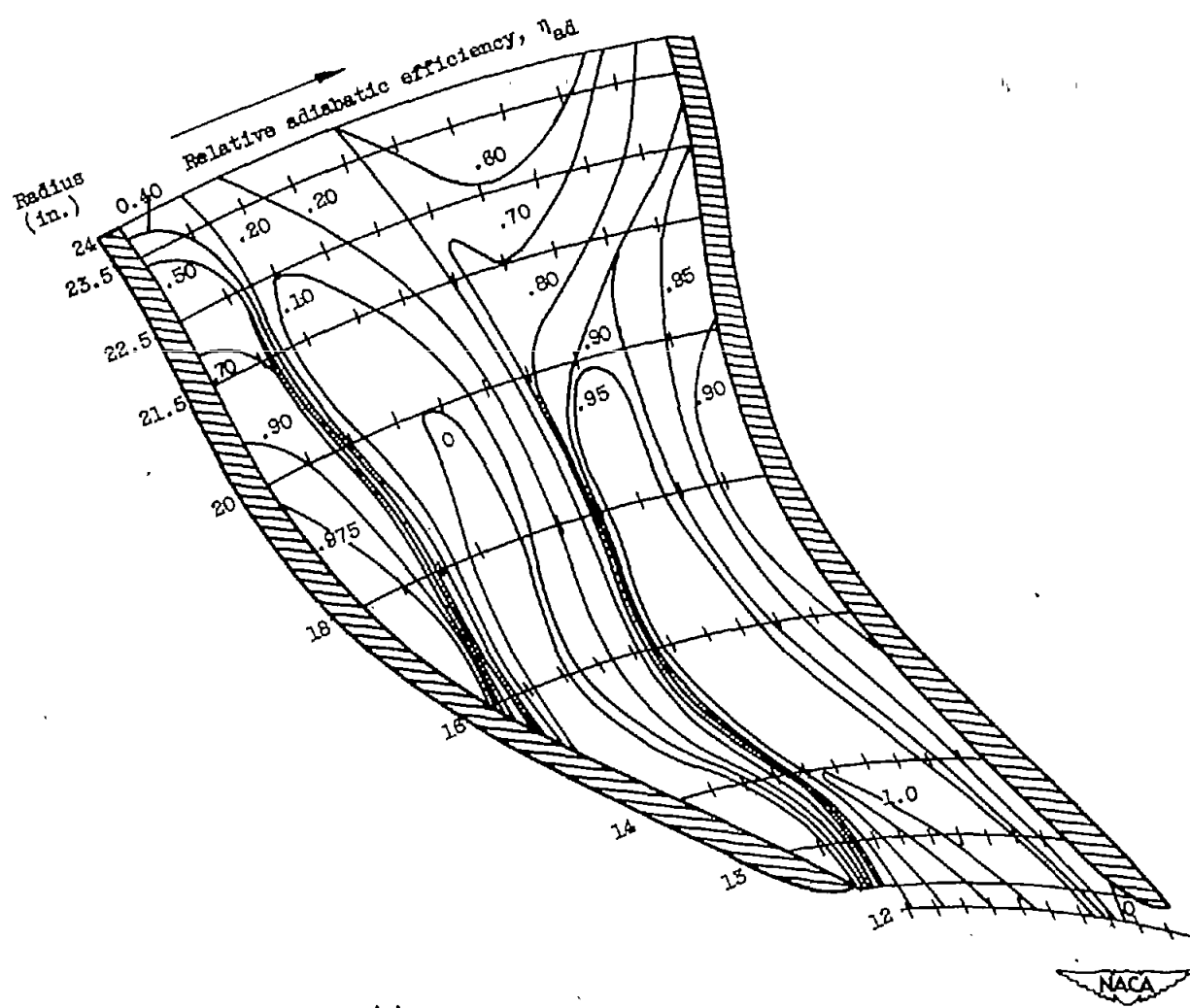
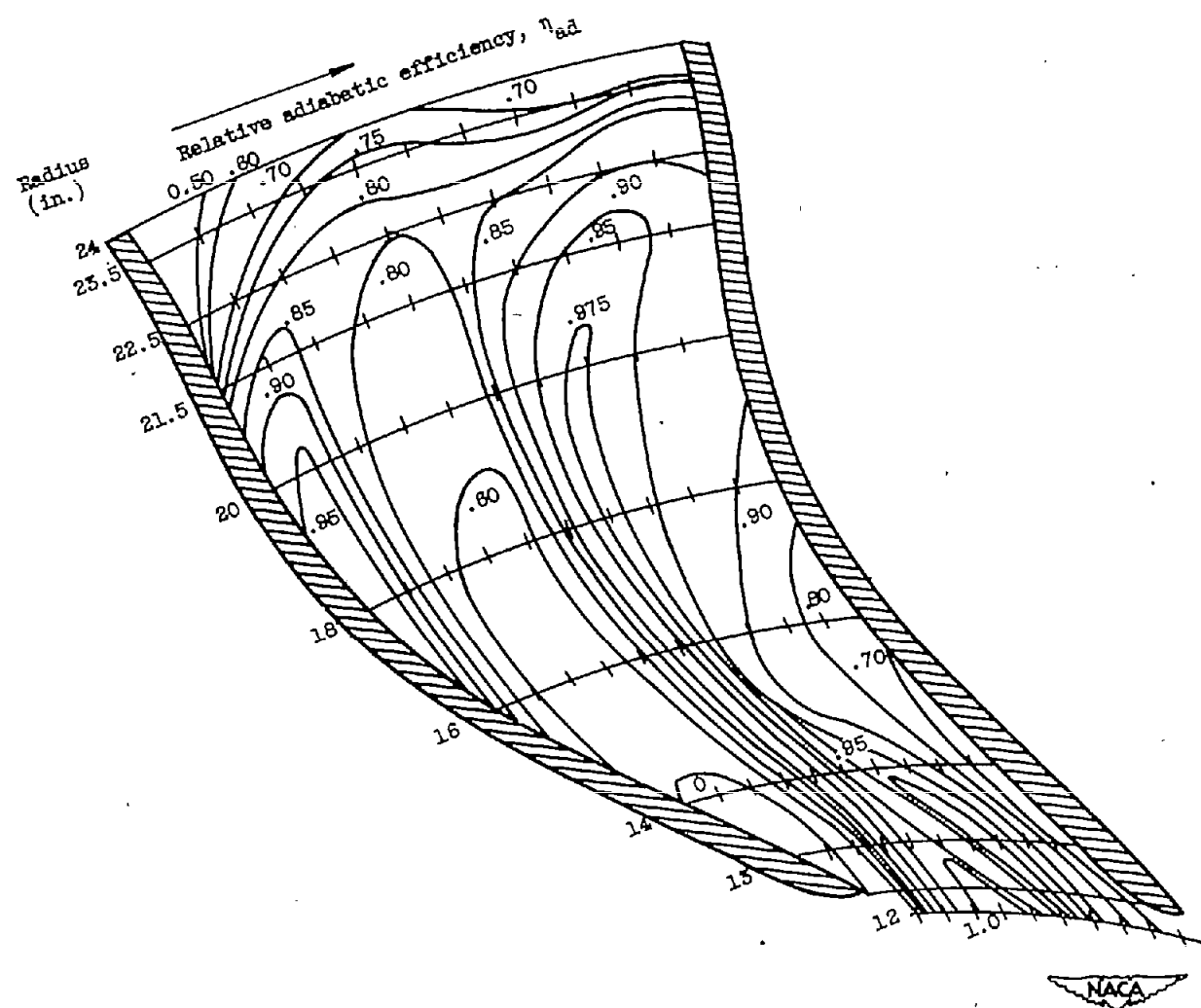


Figure 10. - Relative velocity distribution near blade surfaces for three impeller configurations at corrected weight flow of 26 pounds per second.



(a) Corrected weight flow, 43 pounds per second.

Figure 11. - Relative efficiency distribution throughout modified-hub passage.



(b) Corrected weight flow, 39 pounds per second.

Figure 11. - Continued. Relative efficiency distribution throughout modified-hub passage.

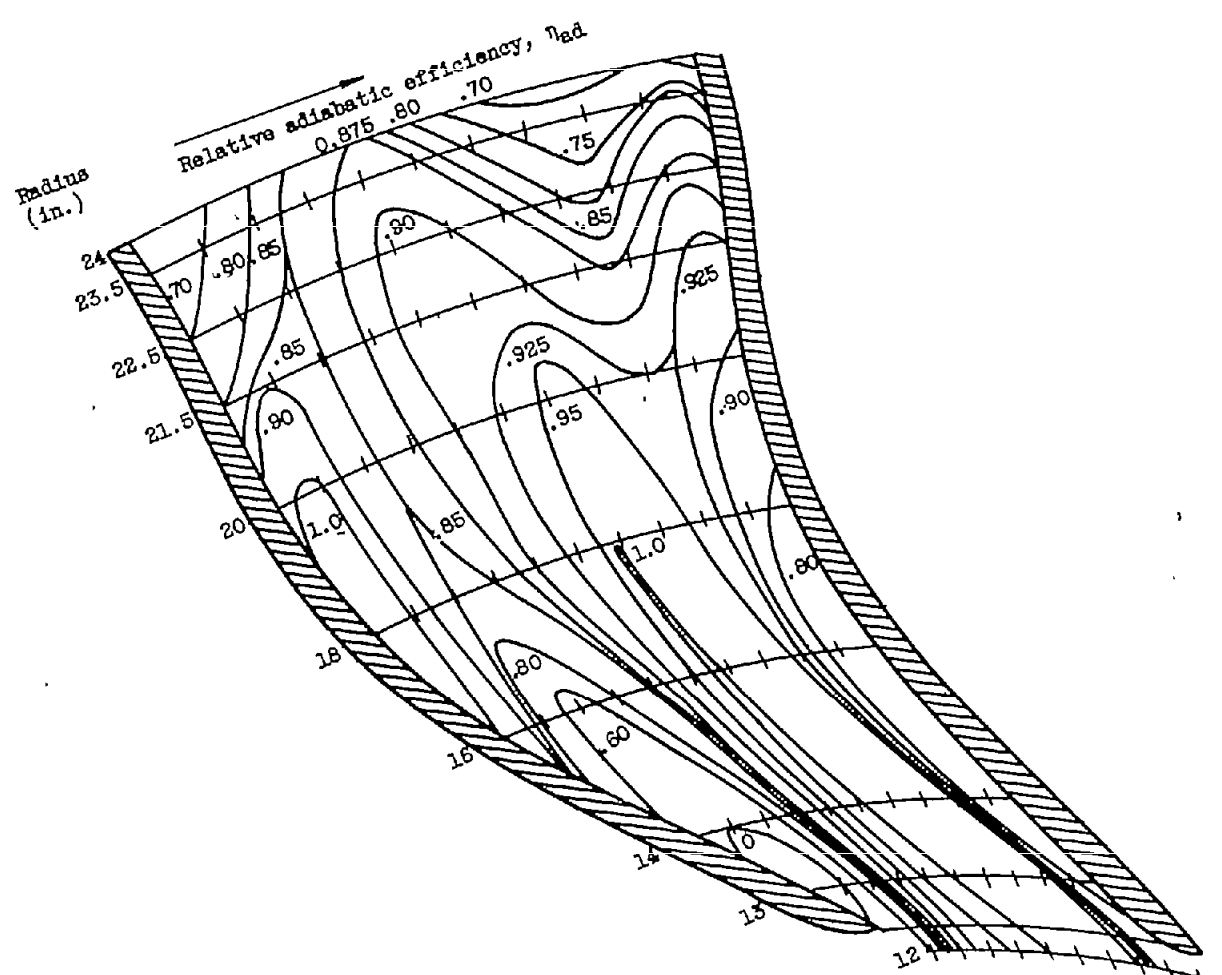
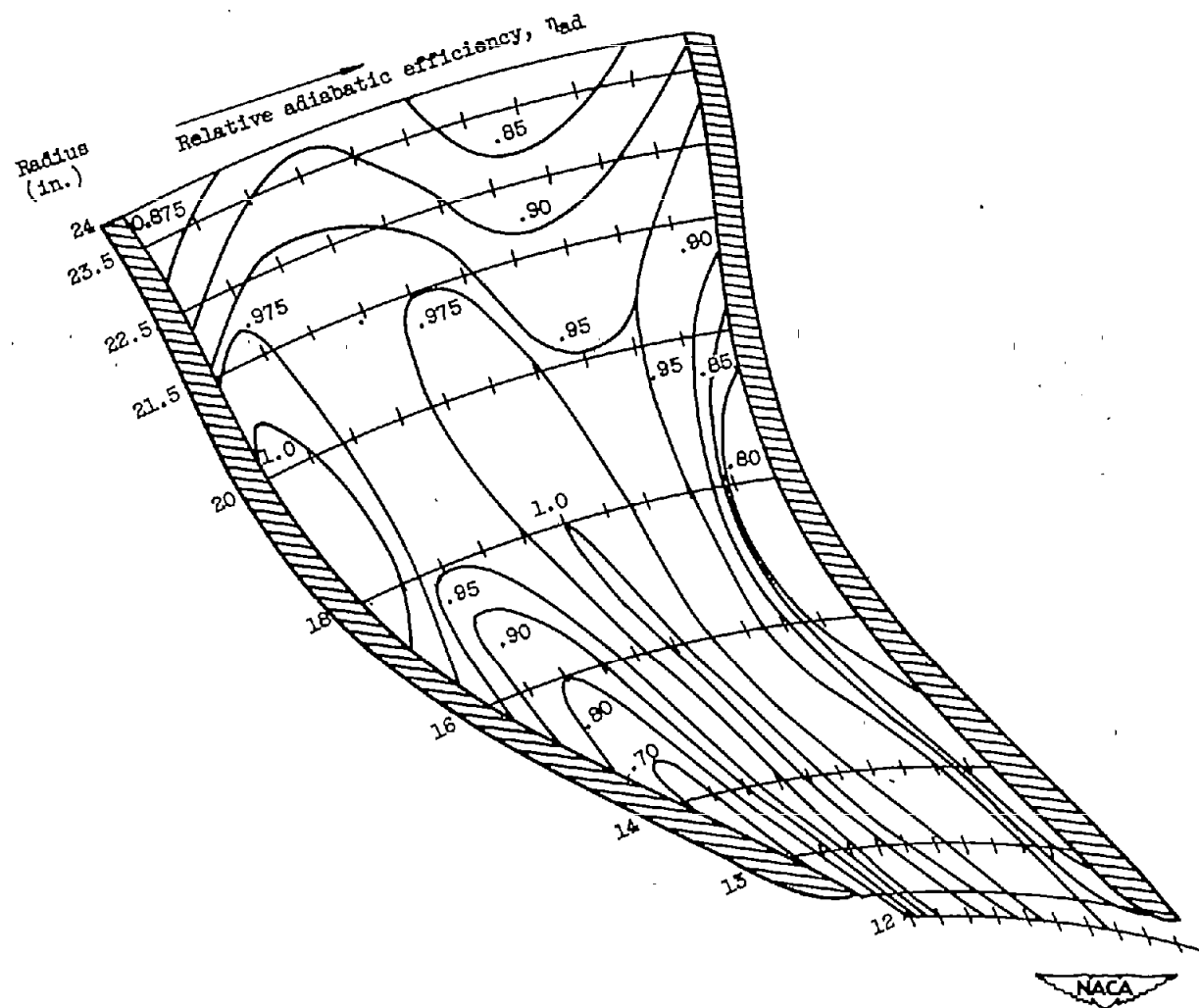
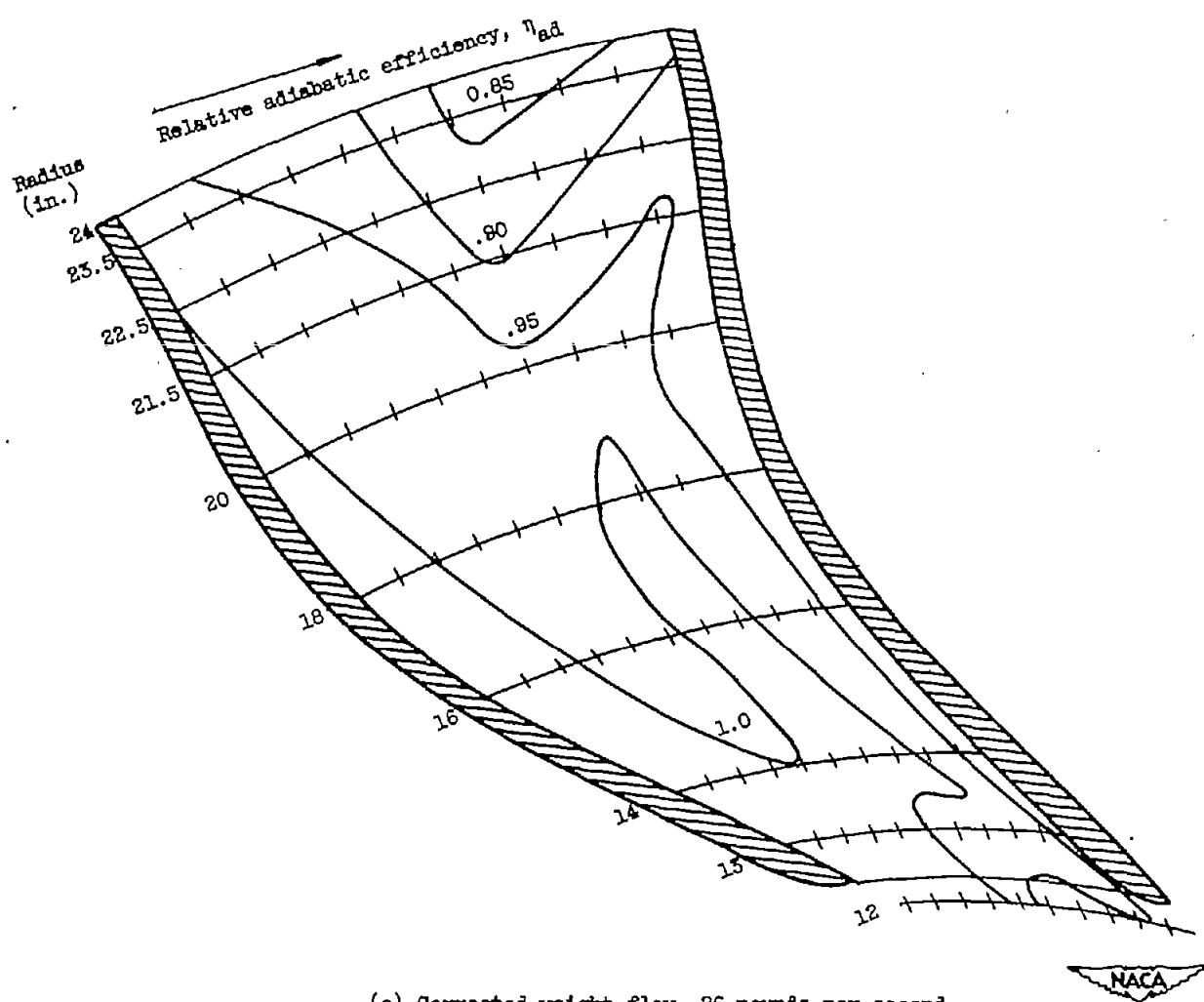


Figure 11. - Continued. Relative efficiency distribution throughout modified-hub passage.



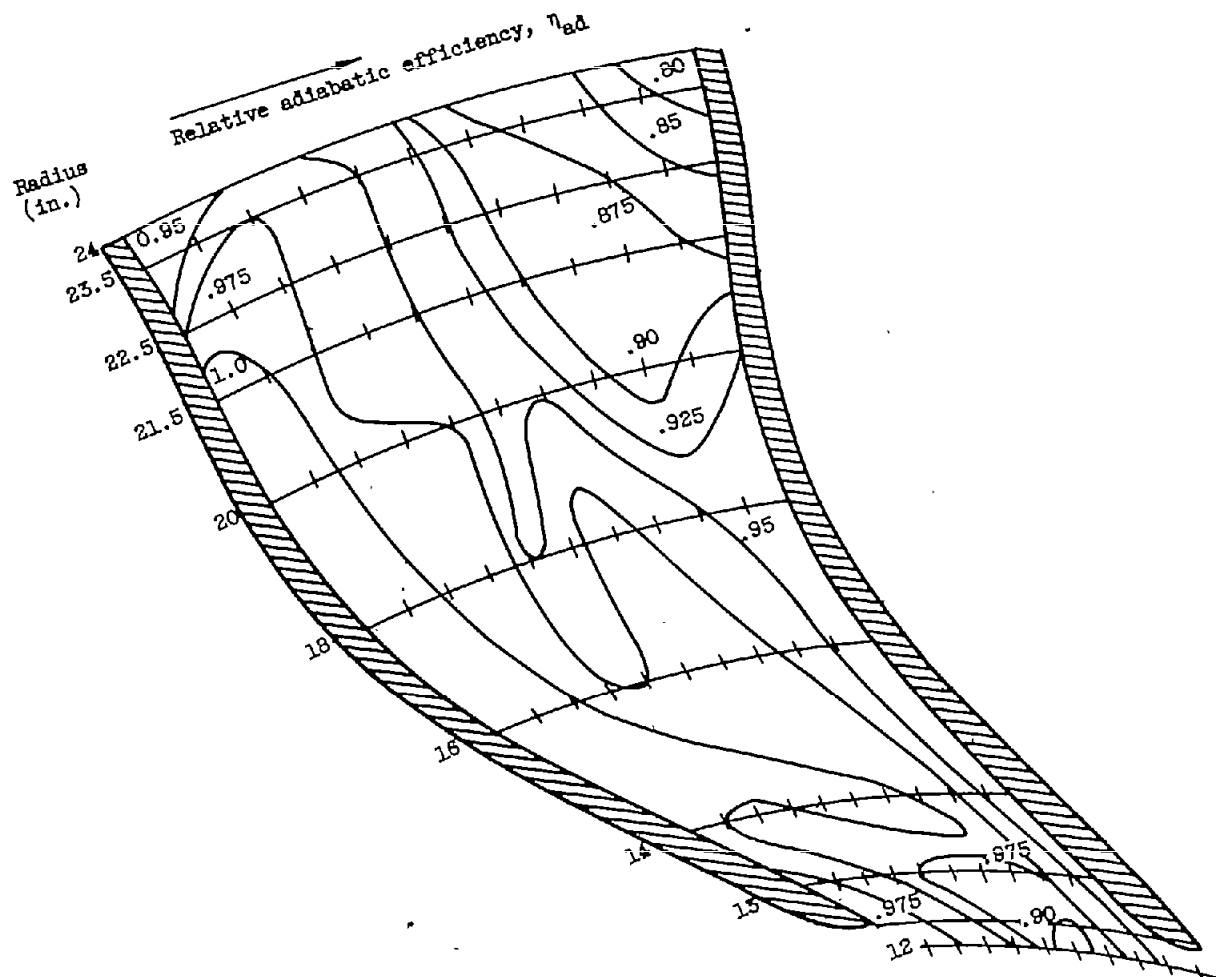
(d) Corrected weight flow, 30 pounds per second.

Figure 11. - Continued. Relative efficiency distribution throughout modified-hub passage.



(e) Corrected weight flow, 26 pounds per second.

Figure 11. - Continued. Relative efficiency distribution throughout modified-hub passage.



(f) Corrected weight flow, 21.5 pounds per second.

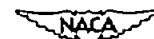
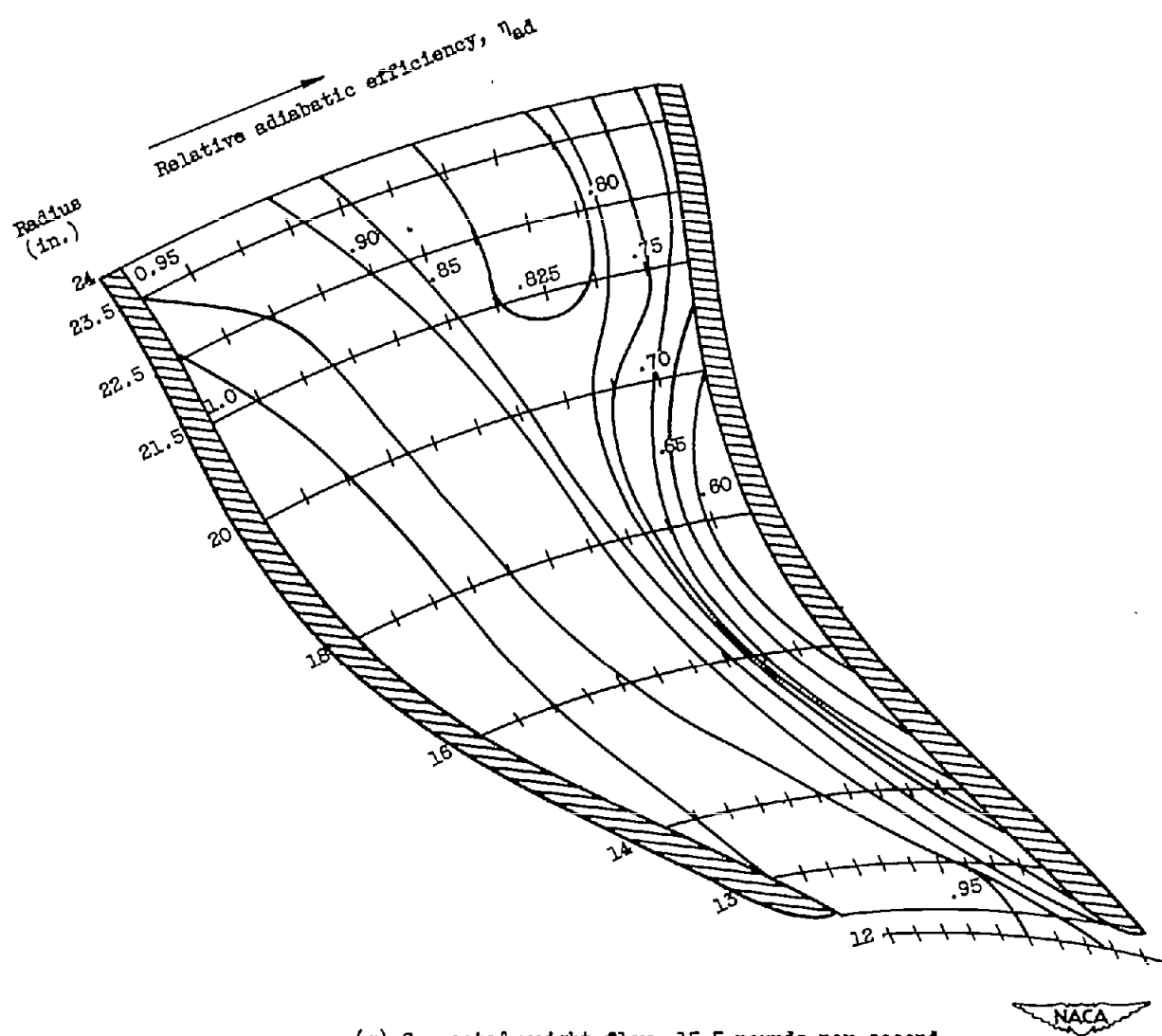
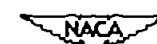
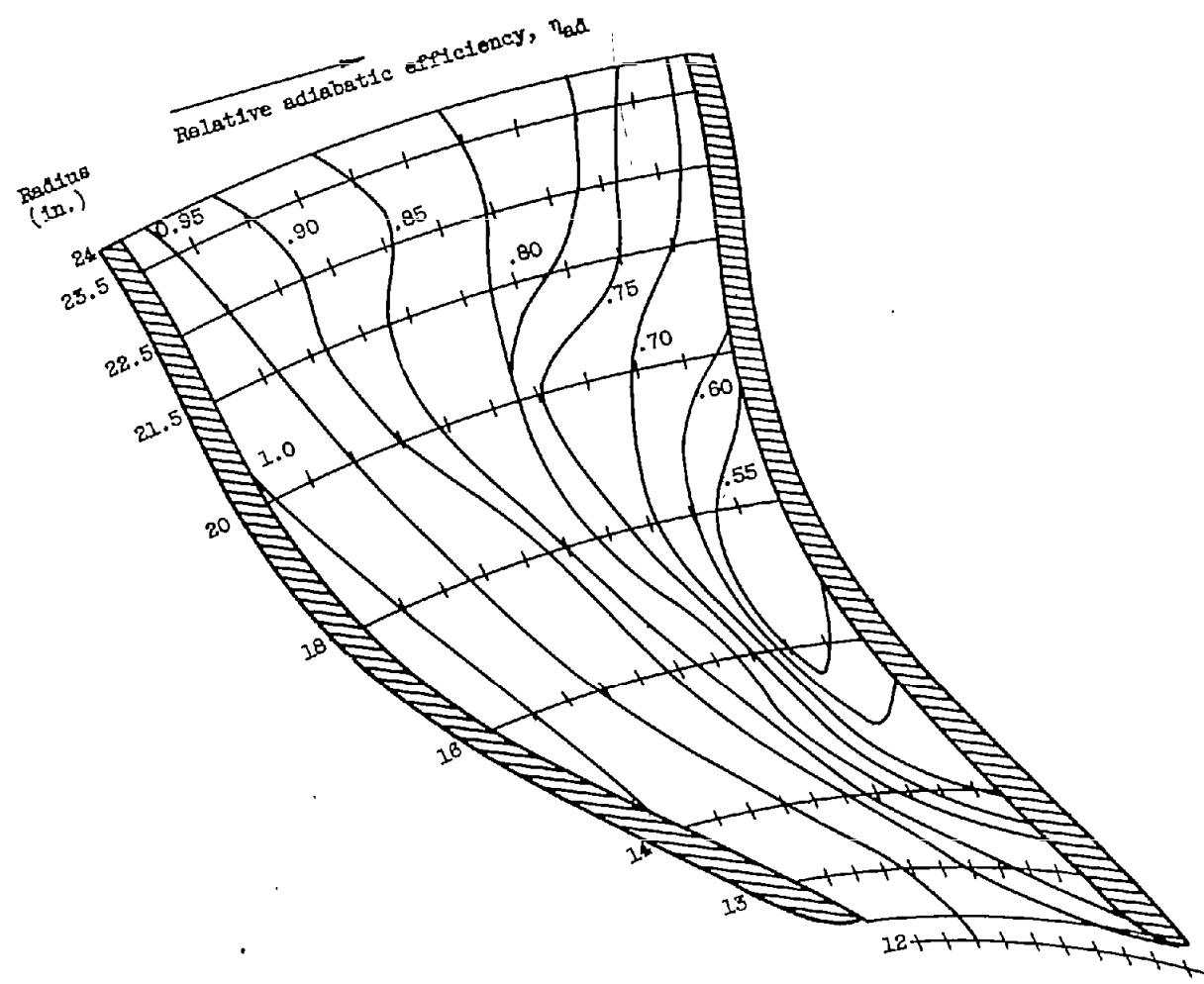


Figure 11. - Continued. Relative efficiency distribution throughout modified-hub passage.



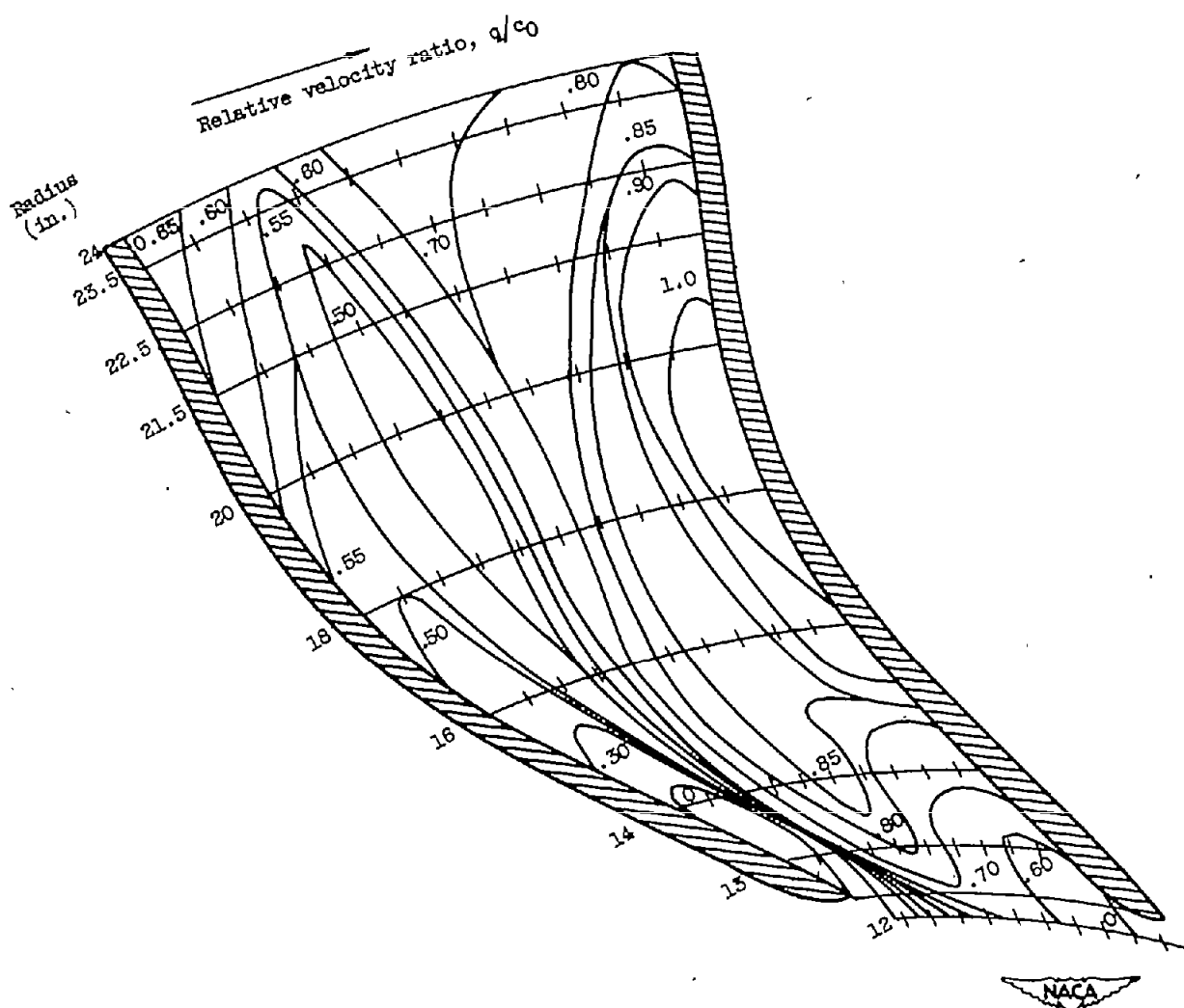
(g) Corrected weight flow, 15.5 pounds per second.

Figure 11. - Continued. Relative efficiency distribution throughout modified-hub passage.



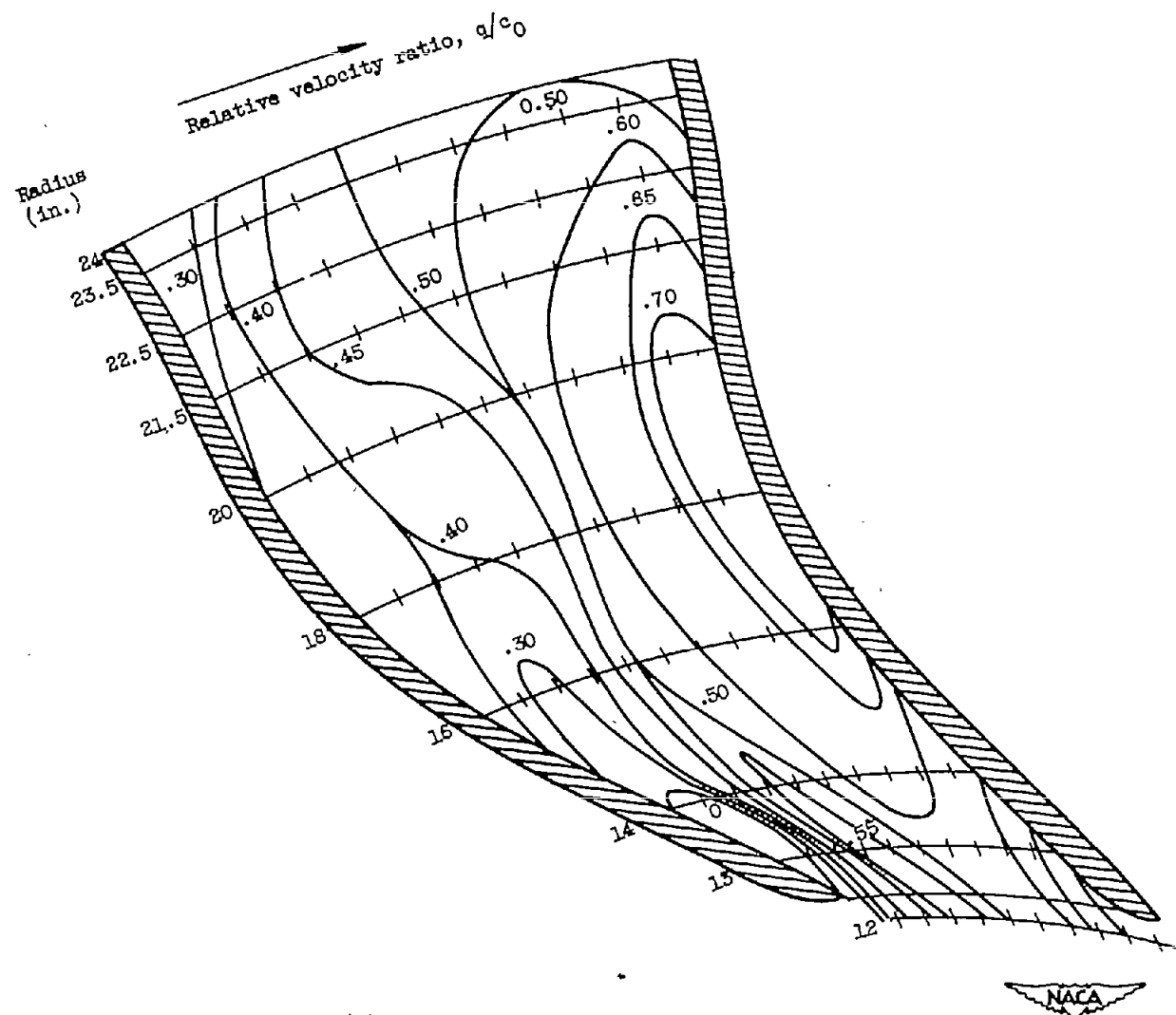
(h) Corrected weight flow, 12.5 pounds per second.

Figure 11. - Concluded. Relative efficiency distribution throughout modified-hub passage.



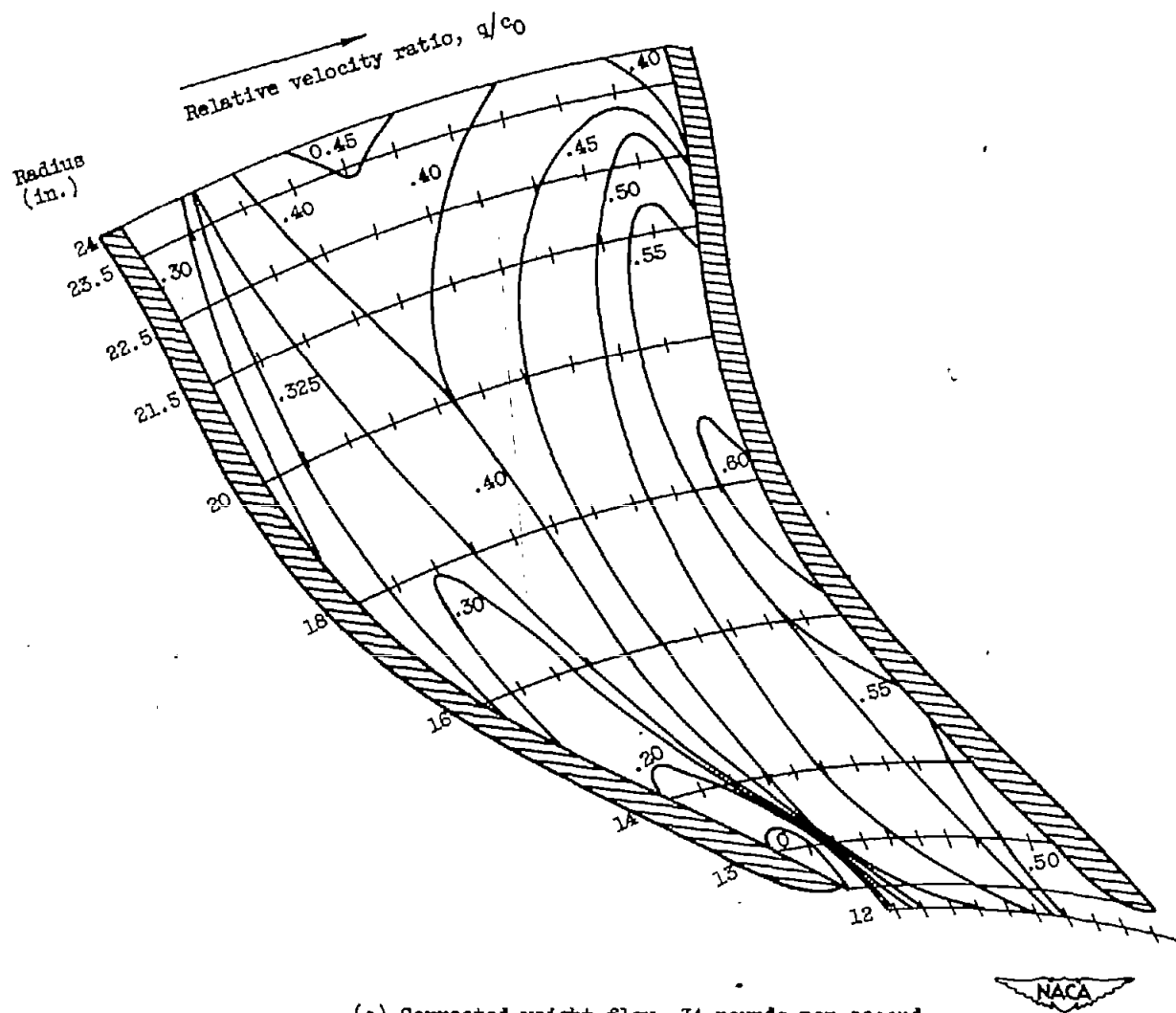
(a) Corrected weight flow, 43 pounds per second.

Figure 12. - Relative velocity distribution throughout modified-hub passage.



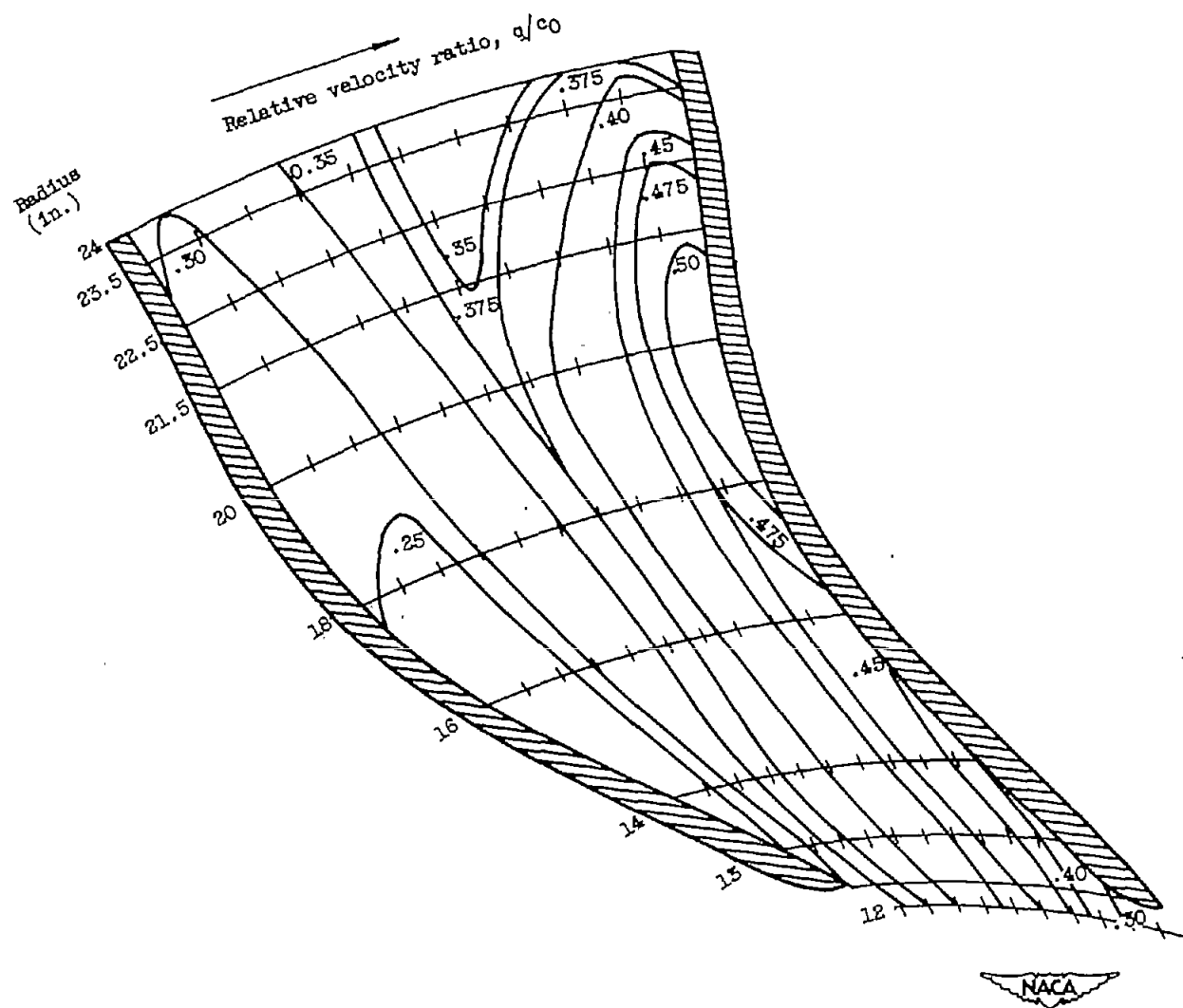
(b) Corrected weight flow, 39 pounds per second.

Figure 12. - Continued. Relative velocity distribution throughout modified-hub passage.



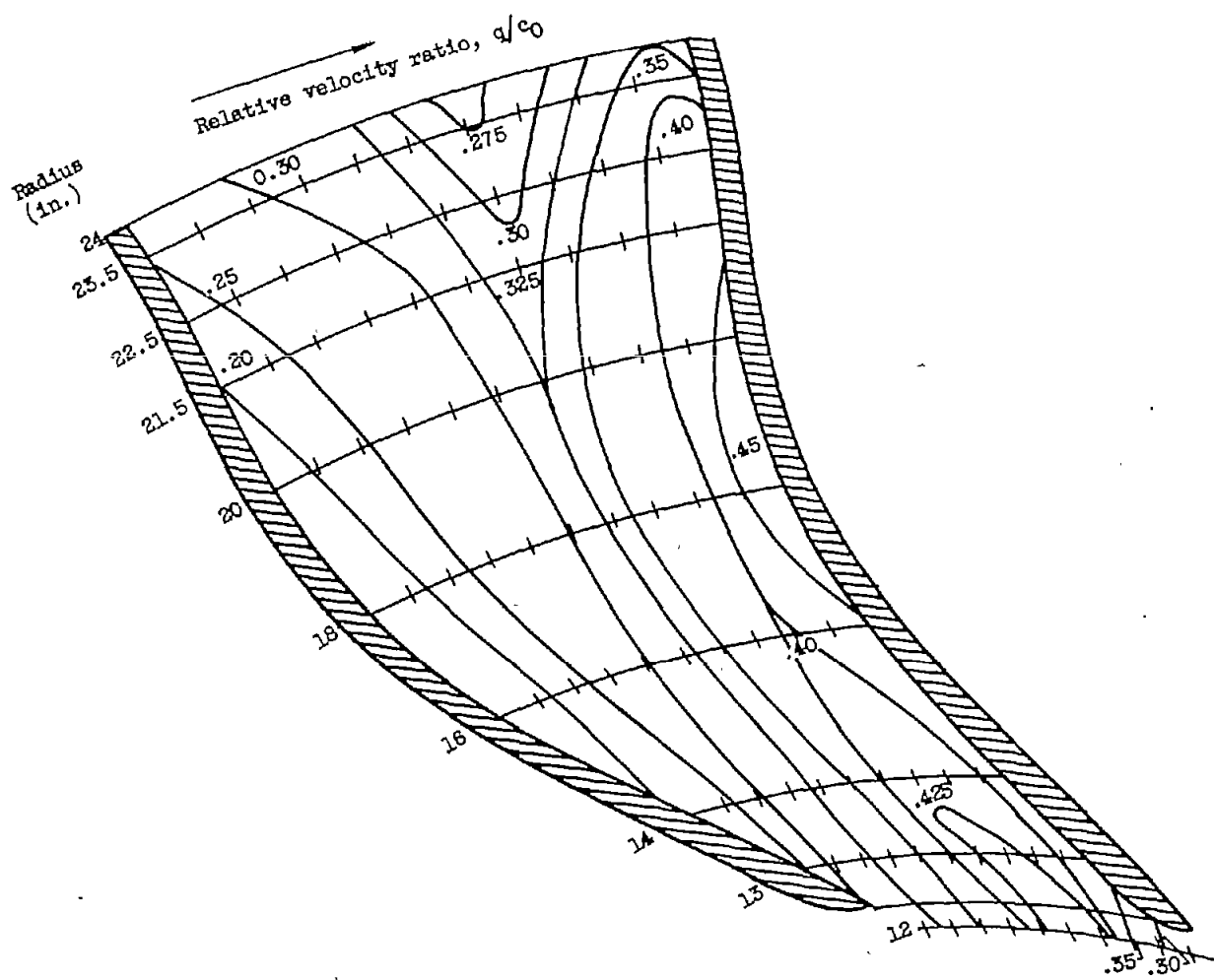
(c) Corrected weight flow, 34 pounds per second.

Figure 12. - Continued. Relative velocity distribution throughout modified-hub passage.



(d) Corrected weight flow, 30 pounds per second.

Figure 12. - Continued. Relative velocity distribution throughout modified-hub passage.



(e) Corrected weight flow, 26 pounds per second.

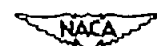
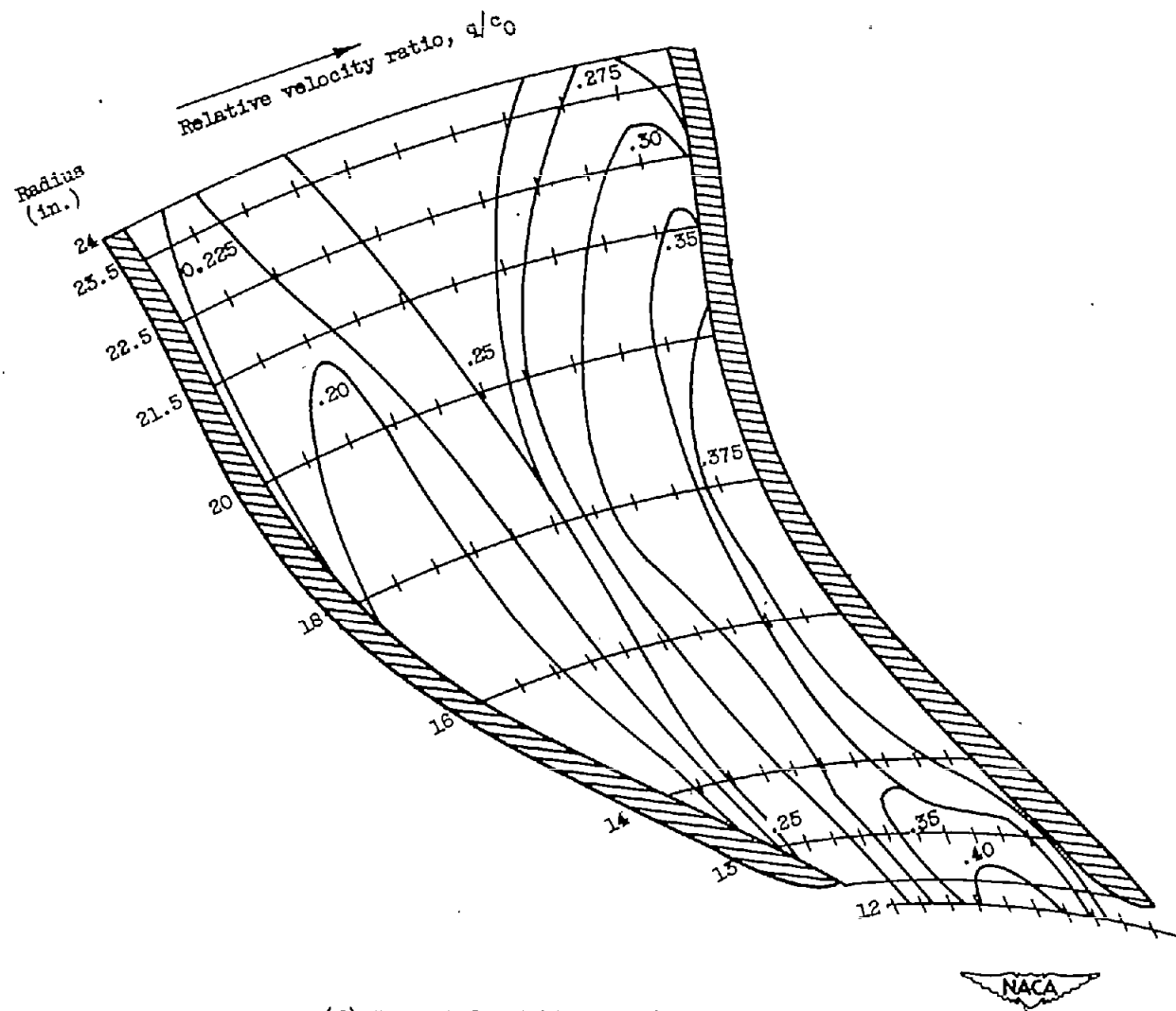
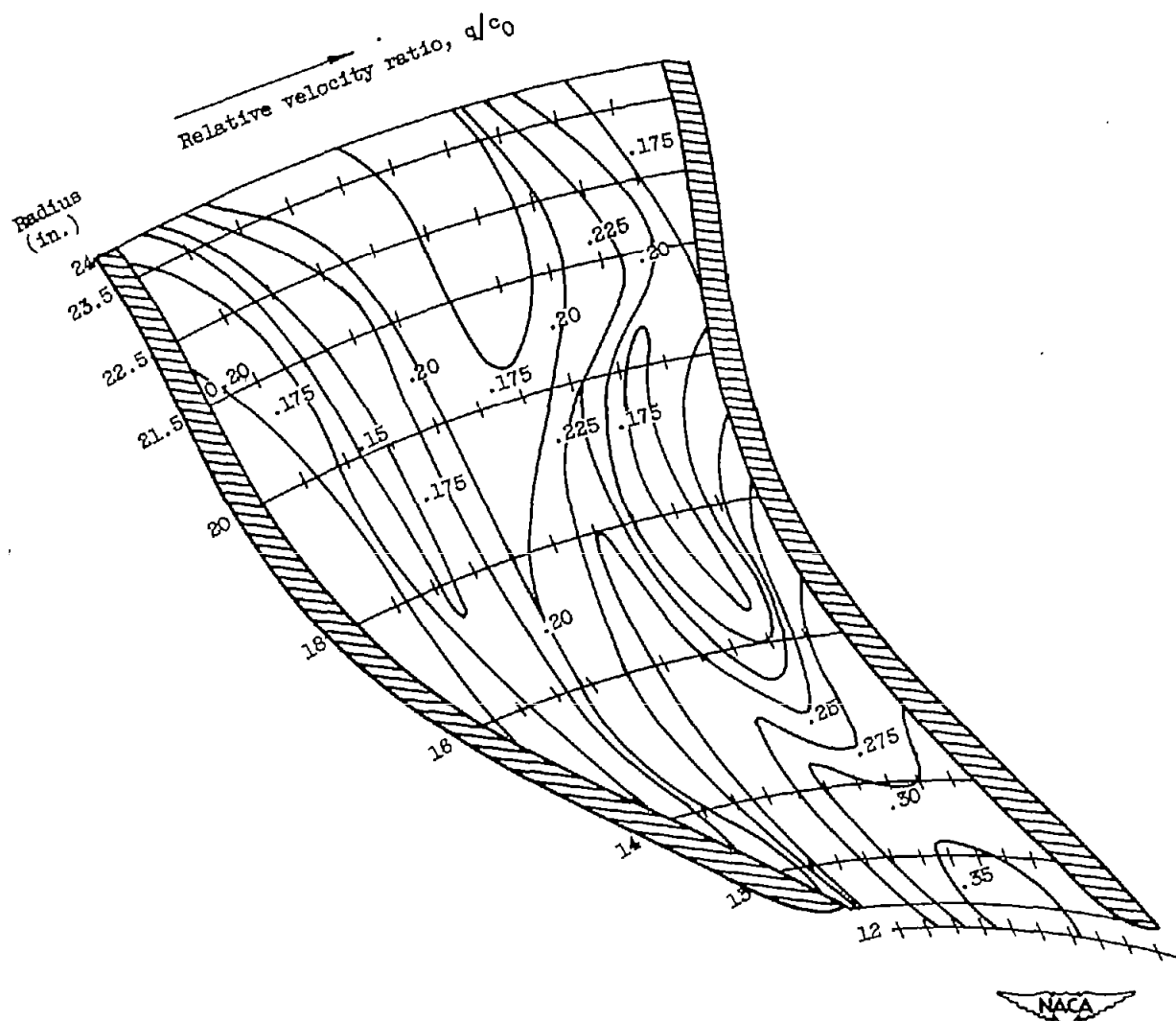


Figure 12. - Continued. Relative velocity distribution throughout modified-hub passage.



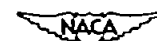
(f) Corrected weight flow, 21.5 pounds per second.

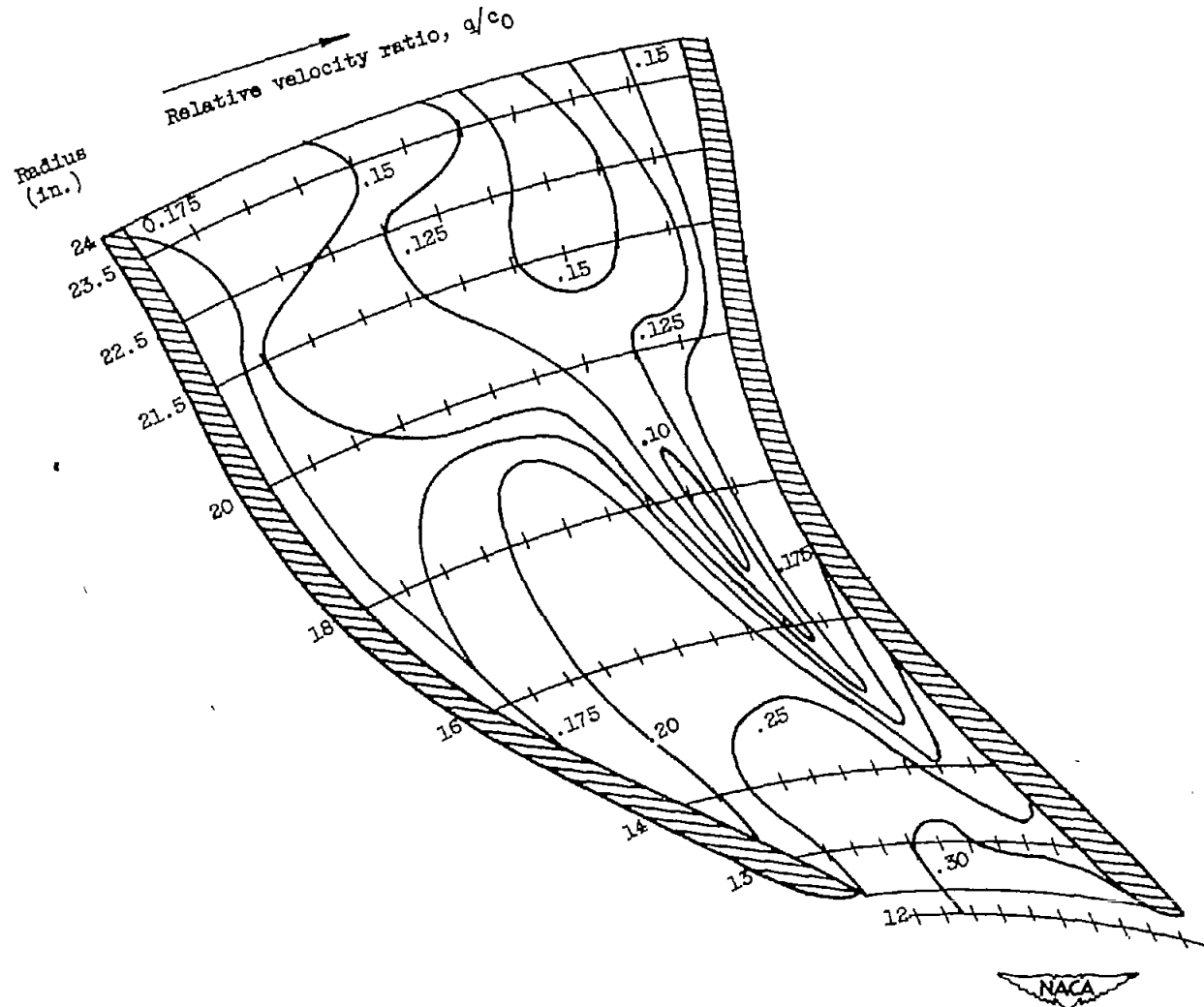
Figure 12. - Continued. Relative velocity distribution throughout modified-hub passage.



(g) Corrected weight flow, 15.5 pounds per second.

Figure 12. - Continued. Relative velocity distribution throughout modified-hub passage.





(h) Corrected weight flow, 12.5 pounds per second.

Figure 12. - Concluded. Relative velocity distribution throughout modified-hub passage.